Journal of the American Heart Association

ORIGINAL RESEARCH

Remote Limb Ischemic Postconditioning Protects Against Ischemic Stroke by Promoting Regulatory T Cells Thriving

Hai-Han Yu, MD*; Xiao-Tong Ma, MD*; Xue Ma, MD; Man Chen, MD; Yun-Hui Chu, MD; Long-Jun Wu, PhD; Wei Wang, MD, PhD; Chuan Qin, MD, PhD; Dai-Shi Tian, MD, PhD

BACKGROUND: Remote limb ischemic postconditioning (RLIPoC) has been demonstrated to protect against ischemic stroke. However, the underlying mechanisms of RLIPoC mediating cross-organ protection remain to be fully elucidated.

METHODS AND RESULTS: Ischemic stroke was induced by middle cerebral artery occlusion for 60 minutes. RLIPoC was performed with 3 cycles of 10-minute ischemia followed by 10-minute reperfusion of the bilateral femoral arteries immediately after middle cerebral artery reperfusion. The percentage of regulatory T cells (Tregs) in the spleen, blood, and brain was detected using flow cytometry, and the number of Tregs in the ischemic hemisphere was counted using transgenic mice with an enhanced green fluorescent protein-tagged Foxp3. Furthermore, the metabolic status was monitored dynamically using a multispectral optical imaging system. The Tregs were conditionally depleted in the depletion of Treg transgenic mice after the injection of the diphtheria toxin. The inflammatory response and neuronal apoptosis were investigated using immunofluorescent staining. Infarct volume and neurological deficits were evaluated using magnetic resonance imaging and the modified neurological severity score, respectively. The results showed that RLIPoC substantially reduced infarct volume, improved neurological function, and significantly increased Tregs in the spleen, blood, and ischemic hemisphere after middle cerebral artery occlusion. RLIPoC was followed by subsequent alteration in metabolites, such as flavin adenine dinucleotide and nicotinamide adenine dinucleotide hydrate, both in RLIPoC-conducted local tissues and circulating blood. Furthermore, nicotinamide adenine dinucleotide hydrate can mimic RLIPoC in increasing Tregs. Conversely, the depletion of Tregs using depletion of Treg mice compromised the neuroprotective effects conferred by RLIPoC.

CONCLUSIONS: RLIPoC protects against ischemic brain injury, at least in part by activating and maintaining the Tregs through the nicotinamide adenine dinucleotide/nicotinamide adenine dinucleotide hydrate pathway.

Key Words: ischemic postconditioning ■ ischemic stroke ■ metabolism ■ regulatory T cells

Ischemic stroke is a growing threat to human health, given its high mortality and morbidity.[1,2] Unfortunately, only a few treatments for acute cerebral infarction have been approved; they include intravenous thrombolysis and vascular recirculation mechanical thrombectomy, which have a narrow time window and limited applicable population.[3–5] Therefore, tremendous efforts have been made to develop more potential therapies.

Research on ischemic postconditioning, a therapeutic procedure with several episodes of sublethal ischemia or reperfusion in primary or distant organs to protect primary organs against ischemic damage, has become increasingly prominent.[6,7] The protective

Correspondence to: Dai-Shi Tian, MD, PhD, or Chuan Qin, MD, PhD, Department of Neurology, Tongji Hospital, Tongji Medical College, Huazhong University of Science and Technology, 1095 Jiefang Avenue, Wuhan, Hubei 430030, P.R. China. E-mail: tiands@tjh.tjmu.edu.cn; chuanqin@tjh.tjmu.edu.cn

Supplementary Material for this article is available at https://www.ahajournals.org/doi/suppl/10.1161/JAHA.121.023077

†H.-H. Yu and X.-T. Ma contributed equally.

For Sources of Funding and Disclosures, see page 15.

JAHA is available at: www.ahajournals.org/journal/jaha

CLINICAL PERSPECTIVE

What Is New?

- Remote limb ischemic postconditioning attenuating ischemic brain injury is partly responsible for an increase in regulatory T cells.
- Remote limb ischemic postconditioning promotes thriving of regulatory T cells by modifying the spectrum of metabolites, especially the decrease of nicotinamide adenine dinucleotide:nicotinamide adenine dinucleotide hydrate ratio.

What Are the Clinical Implications?

- Easily feasible in patients, remote limb ischemic postconditioning has high potential for acute ischemic stroke therapy.
- Modification of nicotinamide adenine dinucleotide:nicotinamide adenine dinucleotide hydrate ratio may have translational implications because of its effects on the abundance of regulatory T cells.

Nonstandard Abbreviations and Acronyms

DEREG	depletion of regulatory T cell
DT	diphtheria toxin
FAD	flavin adenine dinucleotide
MCAO	middle cerebral artery occlusion
NAD$^+$	nicotinamide adenine dinucleotide
NADH	nicotinamide adenine dinucleotide hydrate
RLIPoC	remote limb ischemic postconditioning
Tregs	regulatory T cells

mechanisms underlying ischemic postconditioning have contributed to multiple aspects. Previous studies showed that ischemic postconditioning can improve cerebral blood flow after reperfusion, reduce oxidative stress injury,[8–10] and inhibit inflammatory response after cerebral ischemia.[11,12]

The innate immune responses, including the activation of microglia and neutrophils, play crucial roles in ischemic brain injury; for example, neutrophils have been demonstrated to be involved in the progression of ischemic preconditioning.[13] Adaptive immunity has also been reported to participate in inflammation induced by ischemic stroke.[14] As a specialized subset of T lymphocytes, regulatory T cells (Tregs) play a critical role in maintaining immune tolerance and suppressing the overactivation of the immune system in several inflammatory diseases, including ischemic stroke.[15,16] Tregs orchestrate inflammation via releasing cytokines or direct contact with other immunocytes.[16,17] It has been reported that Tregs can produce interleukin-10, attenuate the infiltration of peripheral inflammatory cells into the peri-infarct area, and suppress astrogliosis after ischemic stroke.[16,18,19] Tregs have also been shown to increase in the blood of stroke patients and experimental stroke animals several days after ischemic stroke.[20,21] The Tregs in the brain were 2-fold among CD4$^+$ T cells within a day after middle cerebral artery occlusion (MCAO).[22] These studies suggested that Tregs in peripheral blood and the central nervous system were involved in the pathological process of ischemic stroke.

Considering these premises, it is reasonable to speculate that remote limb ischemic postconditioning (RLIPoC) can influence the quantity of Tregs in the peripheral immune system, followed by infiltration of the ipsilateral hemisphere after ischemic stroke. Hence, in this study, we explored the influence of RLIPoC on the quantity of Tregs and the underlying mechanisms in an experimental ischemic stroke model. Considering the importance of microglia in the immune system of the central nervous system and the interplay between microglia and Tregs,[16,23] we explored how RLIPoC influences the induction of Tregs and how it influences the thriving interaction of Tregs with microglia.

METHODS

The data that support the findings of this study are available from the corresponding author upon reasonable request.

Animals

Adult male C57BL/6J (wild type) mice (8–10 weeks, 20–25 g) were obtained from Vital River Laboratory Animal Technology Co. Ltd., Beijing, China. The C57BL/6-Tg (Foxp3-DTR/EGFP [enhanced green fluorescence protein]) mice (#32050-JAX, The Jackson Laboratory, Bar Harbor, ME, USA), also known as depletion of regulatory T cell (DEREG) bacterial artificial chromosome transgenic mice, were used to ablate Tregs via the injection of the diphtheria toxin (DT). Fluorescence microscopy was used to detect Tregs in B6129S-Tg (Foxp3-EGFP/icre) mice (#023161, The Jackson Laboratory). The mice were housed in a 12-hour light/dark cycle environment with a 22±1 °C temperature and fed with food and water ad libitum. All animal studies were approved by the Experimental Animal Ethics Committee of Huazhong University of Science and Technology.

Ischemic Stroke Model and Remote Limb Ischemic Postconditioning Procedure

Transient cerebral ischemia was induced by intraluminal occlusion of the right middle cerebral artery for 60 minutes, as described in a previous study.[24] The mice were anesthetized by the inhalation of isoflurane, and right cervical vessels were exposed by making a midline neck incision. The common carotid artery and internal carotid artery were ligated temporarily. The external carotid artery was dissected further distally and coagulated. A nylon suture coated with silicone was inserted into the external carotid artery; the external carotid artery trunk was used as a path to advance the suture into the internal carotid artery and farther into the circle of Willis, effectively occluding the middle cerebral artery. Reperfusion was allowed by nylon suture removal and common carotid artery loosening an hour later. Laser Doppler flowmetry was used to monitor cerebral blood flow (CBF), and the animals that showed a CBF reduction of <75% were excluded.

RLIPoC was performed immediately after the MCAO model. The bilateral femoral arteries were exposed through skin incisions in the hind limbs and carefully dissected from the surrounding facias, femoral veins, and femoral nerves. Ischemia and reperfusion of the hind limbs were controlled by clamping or releasing femoral arteries using microvascular clamps. Three cycles of 10-minute ischemia followed by 10-minute reperfusion of the bilateral femoral arteries were performed immediately after middle cerebral artery reperfusion.

Two hundred and forty-seven wild type mice were made MCAO model, among whom 108 received RLIPoC (MCAO+RLIPoC). Among the 247 wild type mice, 37 mice whose CBF reduction was <75% and 29 mice that died at a different time point after MCAO were excluded from this study. The remaining 181 mice were 78 in the MCAO group, 81 in the MCAO+RLIPoC group, 7 in the MCAO+Tregs group, and 15 in the MCAO+NADH group, respectively. Sixty-two B6129S-Tg (Foxp3-EGFP/icre) mice were made MCAO model, among whom 26 received RLIPoC. Among the 62 B6129S-Tg (Foxp3-EGFP/icre) mice, 11 mice whose CBF reduction was <75% and 8 mice that died at a different time point after MCAO were excluded from this study. The remaining 43 mice were 19 in the MCAO group, 18 in the MCAO+RLIPoC group, and 6 in the MCAO+NADH group, respectively. Ten DEREG mice were made MCAO model. Among the 10 DEREG mice, 2 mice whose CBF reduction was <75% and 2 mice that died at a different time point after MCAO were excluded from this study. The remaining 6 mice were in the MCAO+DT+RLIPoC group. The blood, spleen, and brain tissues were harvested at indicated time points.

Tissue Metabolic Measurements

The multispectral optical imaging system developed by Wuhan National Laboratory for Optoelectronics, Huazhong University of Science and Technology, was used to measure the tissue metabolism of flavin adenine dinucleotide (FAD), Cytaa3-R (cytochrome aa3 in a reduced state), and Cytc-R (cytochrome c in a reduced state) in vivo, as mentioned in a previous study.[25] Three cycles of ischemic postconditioning were performed, the raw images were collected continuously and imported into MATLAB, and a region of interest on claw image was chosen to calculate the changes in the concentrations of FAD, Cytaa3-R, and Cytc-R.

Nicotinamide adenine dinucleotide hydrate (NADH), which oxidizes to nicotinamide adenine dinucleotide (NAD^+), was detected using an NAD^+/NADH assay kit (S0175, Beyotime Biotechnology, Shanghai, China), according to the manufacturer's instructions. Shortly after ischemic postconditioning of the bilateral femoral arteries, blood was collected in a tube with EDTA and the tube was centrifuged for 15 minutes at 3000 rpm (1500*g*), 4 °C, to acquire plasma. In addition, 10 to 20 mg of the gastrocnemius muscle was collected and homogenized with 400 μL of cold lysis buffer in a 1.5 mL Eppendorf tube. The tube was centrifuged for 10 minutes at 12 000*g*, 4 °C, to acquire the supernatant. The total NAD^+/NADH was detected by adding 20 μL of plasma/supernatant to a 96-well plate. To detect only NADH, 20 μL of plasma/supernatant incubated at 60 ℃ for 30 minutes was added to a 96-well plate. Subsequently, 90 μL of alcohol dehydrogenase and 10 μL of chromogenic solution were successively added to the same 96-well plate and incubated at 37 ℃ for 10 and 30 minutes, respectively. Subsequently, the optical density at the wavelength of 450 nm was measured. A standard curve was generated at the same time as the samples to calculate the concentrations of NADH and the total NAD^+/NADH. The concentrations of NAD^+ were derived by subtracting NADH from the total NAD^+/NADH.

Mononuclear Cell Isolation

Regarding the brain tissue, mononuclear cells were isolated by Percoll-gradient centrifugation. Each sample had 2 ischemic hemispheres. The brains were obtained after cardiac perfusion with ice-cold PBS and minced in RPMI-1640 containing DNase I (100 μg/mL, Servicebio, China) and collagenase type II (0.1%, Servicebio, China). After incubation for 30 minutes at 37℃, an equal volume of RPMI-1640 containing 10% fetal bovine serum (FBS) was added to inactivate enzymes. The brains were triturated thoroughly, passed over a 70-μm strainer, centrifuged at 300*g* for 5 minutes at 18 °C, and resuspended with 4 mL of 40% stock isotonic Percoll (90% Percoll+10% 10× Hanks'

Balanced Salt Solution). The cell suspension was carefully transferred into 15-mL centrifuge tubes containing 3 mL of 70% stock isotonic Percoll. The tubes were centrifuged at 637.2*g* at an acceleration of 6 and deceleration of 2 for 30 minutes at 18 °C. The mononuclear cells were collected from the interphase between 40% and 70% of stock isotonic Percoll and washed 2 times with 10 mL of cold PBS.

Peripheral blood mononuclear cells were obtained using Ficoll (17544602, GE Healthcare) by centrifuging at 400*g*, 18℃, for 20 minutes. Splenocytes were isolated after the spleen was homogenized through a 70-μm strainer, followed by red blood cell lysis.

The mononuclear cells were resuspended with flow staining buffer and counted, then used for flow cytometry as described later.

Administration of Drugs

DT (15046A1, List Biologicals Laboratories) was used as previously described.[26] Conditional ablation of Tregs in DEREG mice was achieved by intraperitoneal injection of DT (50 μg/kg body weight) 2 days before the MCAO model. Subsequently, an intraperitoneal dose of DT (10 μg/kg body weight) was administered every other day until day 3 after MCAO.

NADH (NB129, Sigma-Aldrich) was administered by intraperitoneal injection at a dose of 50 mg per mouse within 1 hour after the MCAO model.

Tregs Isolation and Adoptive Transfer

The spleen was isolated from adult mice, and $CD4^+CD25^+$ Tregs were magnetically enriched from single-cell suspensions of splenocytes, using a mouse $CD4^+CD25^+$ Regulatory T Cell Isolation Kit (130-104-453, Miltenyi Biotec, Germany), according to the manufacturer's instructions. Purified $CD4^+CD25^+$ Tregs were transferred intravenously to recipient mice within 1 hour after the MCAO model, with a dose of 1 million per mouse through the tail vein.

Primary Microglia Culture and Oxygen-Glucose Deprivation

Primary microglia were isolated from neonatal C57BL/6J mice as described before.[27,28] The brains were minced and digested in DMEM/F12 containing 0.125% trypsin after removing the meninges. The triturated brains were passed over a 70-μm strainer, centrifuged at 159.3*g* for 10 minutes at 4 °C, resuspended with DMEM/F12 containing 20% FBS, and incubated at 37 ℃ in a humidified atmosphere of 5% CO_2. The culture medium was replaced with DMEM/high-glucose containing 20% FBS every 3 to 4 days for 8 to 10 days. Microglia were isolated by shaking at 6.372*g* at 37 °C for 2 hours. The obtained microglia were seeded into 12-well plates (2×10^5/well) or 24-well plates (3×10^4/well) in DMEM/high-glucose containing 20% FBS for 24 hours before further treatment.

The media were replaced with PBS, and the cells were incubated at 37 ℃ with 5% CO_2 and 1% O_2. After 4 hours, PBS was replaced with DMEM/high-glucose containing 20% FBS, and the Tregs were added to the 12-well plates (2×10^5/well) or 24-well plates (3×10^4/well) to be cocultured with the microglia at a ratio of 1:1. Subsequently, the cells were returned to the normal in a 5% CO_2 incubator. After 20 hours, Zymosan A BioParticles conjugated with Alexa Fluor 488 (Z-23373, Thermo Fisher Scientific, CA, USA) were added to the 24-well plates (12×10^4/well) and cocultured with microglia for 40 minutes at 37 ℃. Finally, the microglia were harvested to perform immunofluorescent staining or quantitative reverse transcription-polymerase chain reaction as described subsquently.

Flow Cytometry

The cells were incubated with anti-CD16/CD32 (KT1632, Invitrogen, Thermo Fisher Scientific) for 15 minutes at 4 ℃. Single-cell suspensions of splenocytes and peripheral blood mononuclear cells were stained with CD4 fluorescein isothiocyanate (100510, BioLegend, San Diego, CA, USA) and CD25 PE (102007, BioLegend). Mononuclear cells isolated from the brains were stained with CD3e PerCP-Cyanine5.5 (45-0031-82, eBioscience, San Diego, CA, USA), CD4 fluorescein isothiocyanate (11-0041-82, eBioscience,), CD8a PE-Cyanine7 (25-0081-82, eBioscience), and CD25 APC (17-0257-42, eBioscience) for 30 minutes at 4℃. Intracellular staining with Foxp3 APC (17-5773-82, eBioscience) for splenocytes and peripheral blood mononuclear cells and Foxp3 PE (12-4777-42, eBioscience) for mononuclear cells isolated from brains was followed by incubation for 30 minutes at 4℃ after cell fixation and permeabilization using the Foxp3/Transcription Factor Staining Buffer Set (562574, BD Pharmingen Inc., CA, USA) according to the manufacturer's instructions. Finally, data were acquired with an LSRII cytometer (BD Biosciences, San Jose, CA, USA) and analysis was performed using FlowJo (TreeStar, Ashland, OR, USA).

Immunofluorescent Staining

Immunofluorescence was described previously.[28] Briefly, brain slices and adherent cells were fixed in 4% paraformaldehyde for 15 minutes, washed 3 times in PBS, and then permeabilized by 0.25% Triton-X100 in PBS. After blocking with 10% bovine serum albumin for 1 hour at room temperature, slices or cells were incubated with primary antibodies overnight at 4℃, followed by corresponding secondary antibody incubation for 1 hour in the dark at room temperature. Finally, antifade mounting medium with DAPI (P0131, Beyotime

Biotechnology, Shanghai, China) was used to cover slices. Primary antibodies included NeuN (neuronal nuclei; 94403, Cell Signaling Technology, Inc., MA, USA), Cleaved-caspase3 (9664, Cell Signaling Technology, Inc.), Iba-1 (019-19741, Wako Pure Chemical Industries, Ltd., Osaka, Japan), Iba-1 (234004, Synaptic Systems, Göttingen, Germany), MAP2 (17490-1-AP, proteintech, Wuhan, China), CD206 (AF2535, R&D Systems, Minneapolis, MN, USA), CD16/CD32 (553142, BD Pharmingen Inc., CA, USA), major histocompatibility complex II (14-5321-82, eBioscience), and Arg-1 (sc-271430, Santa Cruz Biotechnology, Dallas, TX, USA). Secondary antibodies labeled with Alexa Fluor 488, Cy3, were purchased from Jackson ImmunoResearch Laboratories, with a dilution of 1:200. Images were acquired by confocal microscopy (FV1200, Olympus, Japan). Three to 4 microscopic fields in the border of infarct were randomly captured for quantitative analysis. The border of infarct was determined by the accumulation and morphology of Iba-1$^+$ microglia/macrophages. The percentage of double positive cells in Iba-1$^+$ cells was analyzed by a blinded observer.

Terminal Deoxynucleotidyltransferase-Mediated Biotin–Deoxyuridine Triphosphate Nick-End Labeling Staining

A TUNEL (terminal deoxynucleotidal transferase–mediated biotin–deoxyuridine triphosphate nick-end labeling) staining kit (11684817910, Roche Holding AG, Basel, Switzerland) was used according to the manufacturer's instructions. Briefly, brain slices were fixed in 4% paraformaldehyde for 15 minutes, washed 3 times in PBS, and then antigen retrieval was performed using Citrate Antigen Retrieval Solution (P0081, Beyotime Biotechnology, Shanghai, China). After permeabilizing and blocking by 5%-bovine serum albumin-0.25% Triton-X100 in PBS for 30 minutes at room temperature, slices were incubated with a mixture of Enzyme Solution and Label Solution (1:9) for 1 hour at 37 °C. Slices were incubated with primary antibody NeuN (24307, Cell Signaling Technology, Inc.) overnight at 4 ℃ after washing 3 times in PBS. The remaining steps were the same as in immunofluorescent staining.

Reverse Transcription-Polymerase Chain Reaction

Trizol (15596026, Invitrogen, Thermo Fisher Scientific) was used to extract total RNA from the primary microglia. A 20-μL reaction system containing 500 ng RNA was used for reverse transcription, following the manufacturer's instructions of PrimeScript RT Master Mix (RR036A, Takara Bio Inc., Shiga, Japan). Quantitative polymerase chain reaction was performed using qPCR SYBR Green Master Mix (11201ES08, Yeasen Biotech [Shanghai] Co., Ltd, Shanghai, China) with specific primers, under a reaction condition of 95℃ for 5 minutes, and 95℃ (10 seconds) with a subsequent 60℃ (30 seconds) for 40 cycles. Related primer sequences were β-actin (Forward, 5′- TGGAATCCTGTGGCATCCATGA-3′, Reverse, 5′-AATGCCTGGGTACATGGTGGTA-3′), iNOS (inducible nitric oxide synthase; Forward, 5′-GCTTGTC TCTGGGTCCTCTG-3′, Reverse, 5′-CTCACTGGGACAG CACAGAA-3′), TNF-α (tumor necrosis factor-alpha; Forward, 5′-ACGGCATGGATCTCAAAGAC-3′, Reverse, 5′-AGATAGCAAATCGGCTGACG-3′), CD86 (Forward, 5′-GACCGTTGTGTGTGTTCTGG-3′, Reverse, 5′-GATGA GCAGCATCACAAGGA-3′), Spp1 (secreted phosphoprotein 1; Forward, 5′-CAGAATCTCCTTGCGCCACA-3′, Reverse, 5′-TGGAGTGAAAGTGTCTGCTTGT-3′), interleukin-1β (Forward, 5′-TGTCTTGGCCGAGGACTAA GG-3′, Reverse, 5′-TGGGCTGGACTGTTTCTAATGC-3′), CD68 (Forward, 5′-GGGCTCTTGGGAACTACACG-3′, Reverse, 5′-GGATGGGTACCGTCACAACC-3′), and Lgals3 (Forward, 5′-CAGTGAAACCCAACGCAAAC A-3′, Reverse, 5′-CTCAAAGGGGAAGGCTGACT-3′). Primer specificity and cDNA quality were evaluated by BLAST and fusion curve. β-actin was used as an internal reference, and the target gene expression level was analyzed using the $2^{-\Delta\Delta CT}$ method.

Measurement of Infarct Volume

Infarct volume was assessed by magnetic resonance imaging (MRI) or MAP2 staining. A 3-Tesla magnetic resonance imaging was used to evaluate the infarct volume. Coronal magnetic resonance imaging of mice brain were continuously acquired, for a total of 16 slices (1 mm/slice). The infarct volume was calculated using total infarct area (mm^2) to multiply by 1 mm. As to MAP2 staining, 7 equally spaced (0.8 mm) coronal brain slices encompassing the infarct region were acquired, and the infarct volume was calculated using total infarct area of these 7 brain slices (mm^2) to multiply by 0.8 mm.

Behavioral Tests

The neurological function was measured using the modified Neurological Severity Score as described before.[29]

Statistical Analysis

Data were presented with box plots or mean±SEM. GraphPad Prism software (version 7.0) was used for statistical analyses. Kolmogorov-Smirnov or Shapiro-Wilk normality test were performed to check the normality, and $P \geq 0.05$ conferred the data passed the normality test. If the data passed the normality test, the difference between both groups was assessed by Student *t* test; otherwise Mann-Whitney

test was performed. As to the comparison of differences among multiple groups, 1-way ANOVA was used when the data passed the normality test; otherwise Kruskal-Wallis test was performed. Differences in means across groups with repeated measurements over time were analyzed using 2-way ANOVA. When ANOVA or Kruskal-Wallis test showed significant differences, pair-wise comparisons were tested using post hoc Bonferroni's test or Dunn's test, respectively. $P \leq 0.05$ was considered statistically significant.

RESULTS

RLIPoC Reduced Neuronal Apoptosis and Improved Neurological Outcomes After MCAO

Neuroprotective effects have been observed for remote ischemic postconditioning in brain injury disorders.[9,30,31] In the present study, neuronal apoptosis was evaluated by immunofluorescent co-staining of cleaved-caspase3 and NeuN. RLIPoC reduced neuronal apoptosis after MCAO, especially on early stage (Figure 1A). The decrease of neuronal apoptosis was functionally relevant, as neurologic deficits were significantly ameliorated with a reduction of the modified Neurological Severity Score score, in the RLIPoC group than in the MCAO group (Figure 1B). Besides, protection from RLIPoC in MCAO mice was also indicated by smaller infarct volumes on day 1 and 3 after MCAO (Figure 1C and 1D).

Taken together, these results indicate that RLIPoC exhibits neuroprotective effects after MCAO in mice.

RLIPoC Induces Peripheral Tregs Abundance and Tregs Infiltration in the Brain After MCAO

Previous studies reported that inflammation inhibition underlies neuroprotection of ischemic postconditioning[13,32] and that T lymphocytes were also susceptible to remote ischemic postconditioning.[33] Interestingly, we found that RLIPoC enhanced the ratio of spleen mass to body weight on day 3 after MCAO (Figure S1), suggesting that immunocyte activation might be involved in RLIPoC. We next detected whether Tregs, an important type of anti-inflammatory immunocytes, was affected by RLIPoC. The influence of RLIPoC on peripheral Tregs abundance was first assessed in the spleen and blood using flow cytometry in this study. We observed that Tregs ($CD4^+CD25^+Foxp3^+$) percentage among $CD4^+$ T cells was elevated both in the blood and spleen on day 3 in the RLIPoC group than in the MCAO group (Figure 2A and 2B). The frequencies of Tregs in the ipsilateral hemisphere were also affected by RLIPoC, with a trend of increasing on day 3 after MCAO (Figure 2C). Consistent with the results from flow cytometry, the number of $Foxp3^+$ Tregs increased in areas surrounding the core of infarct in the RLIPoC group mice (Figure 2D). These data suggest that RLIPoC increased Tregs abundance in the blood, spleen, and ipsilateral hemispheres after MCAO.

RLIPoC Induce Tregs Increase Via Modulating Metabolite Concentrations In Vivo

RLIPoC with repeated episodes of ischemia/reperfusion was obviously followed by subsequent changes of metabolism. T cells were susceptible to the metabolic environment, and metabolic disorders can modify the spectrum of T cell subsets.[34,35] Meanwhile, Tregs seemed to have natural resistances to metabolically challenging milieu. In condition contents of limited nutrients, such as the tumor tissues or ischemic microenvironment, Tregs were often thriving and functionally unaffected.[35–38] Therefore, we next monitored the metabolic status of hind limbs that suffered from RLIPoC using a multispectral optical imaging system, which could conduct real-time measurements for several metabolites in vivo.[25] Consistent with previous research,[39] clamping the femoral artery robustly decreased the level of FAD in the ischemic region of the hind limb, in comparison with that at baseline. Reperfusion resulted in rapid recovery of the FAD level (Figure 3A). Notably, the level of FAD decreased progressively from the first to the third cycle of RLIPoC, with a trend curve shown in Figure 3A. Some other metabolites, such as Cytaa3-R and Cytc-R, exhibited a contrary trend to FAD.

The changes of FAD were opposite to NADH,[39] a metabolite with a oxidation state of NAD^+, both involved in the regulation of Tregs.[35,40,41] To investigate changes of NAD^+/NADH, plasma and regional muscle tissue of the hind limb were collected immediately after RLIPoC and detected using an NAD^+/NADH assay kit. The results revealed that the levels of NADH were upregulated both in ischemic conditioning muscle and circulating plasma after RLIPoC, accompanied by a reduction of NAD^+ concentration and subsequent NAD^+:NADH ratio (Figure 3B and 3C). As such, we hypothesized that the imbalance of NAD^+:NADH might contribute to the Tregs increase after RLIPoC. Therefore, NADH was administered within 1 hour after the MCAO model (Figure 3D). After 3 days, Tregs frequencies were evaluated in the spleen and blood using flow cytometry, and results showed that NADH (intraperitoneal 50 mg/mouse)

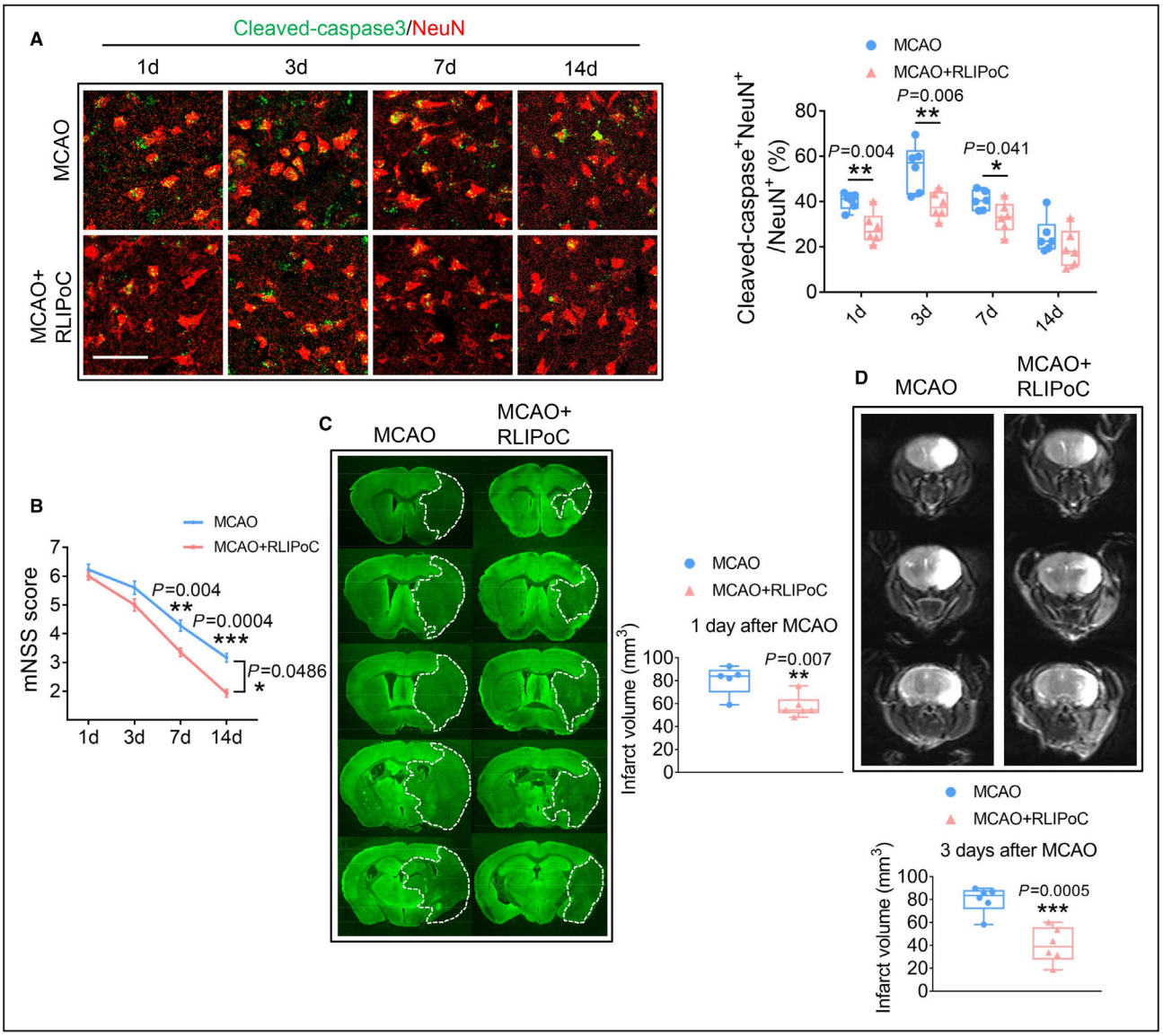

Figure 1. RLIPoC confers neuroprotection after brain ischemic stroke.
A, Neuronal apoptosis was assessed by immunofluorescent staining of Cleaved-caspase3 and NeuN on days 1, 3, 7, and 14 after MCAO. Representative confocal images of coronal sections are labeled with Cleaved-caspase3 and NeuN; quantitative analysis of NeuN and Cleaved-caspase3 double positive cells are shown in the histogram. Scale bar=50 μm. Student *t* test, **P*<0.05, ***P*<0.01 vs MCAO. n=6 per group. **B**, Neurological function was accessed by modified Neurological Severity Score (mNSS) at different time points after MCAO. Two-way ANOVA repeated measurement, **P*<0.05, ***P*<0.01, ****P*<0.001 vs MCAO. n=25 to 50 in each group. **C**, Infarct volume was measured by MAP2 immunostaining at 1 day after MCAO. Student *t* test, ***P*<0.01 vs MCAO. n=5 to 6 per group. **D**, Representative magnetic resonance images and quantification of infarct volume at 3 days after MCAO. Student *t* test, ****P*<0.001 vs MCAO. n=6 per group. MCAO indicates middle cerebral artery occlusion; mNSS, modified Neurological Severity Score; NeuN, neuronal nuclei; and RLIPoC, remote limb ischemic postconditioning.

treatment can mimic the influence of RLIPoC on Tregs and increase the percentage of Tregs in $CD4^+$ cells, 20 mg/mouse with no obvious influence on Tregs abundance (Figure 3E, Figure S2). Similarly, the number of Tregs surrounding the core of infarct in the brain was also elevated on day 3 after NADH administration (Figure 3F).

Taken together, these results elucidated that RLIPoC might stimulate Tregs to thrive after MCAO through orchestrating metabolic modification, such as downregulating the ratio of NAD^+:NADH.

RLIPoC-Induced Neuroprotection Against MCAO was Mediated by Increasing Tregs

Considering that Tregs could ameliorate brain injury after ischemic stroke,[18,42] and the aforementioned results indicated that RLIPoC can induce Tregs increase,

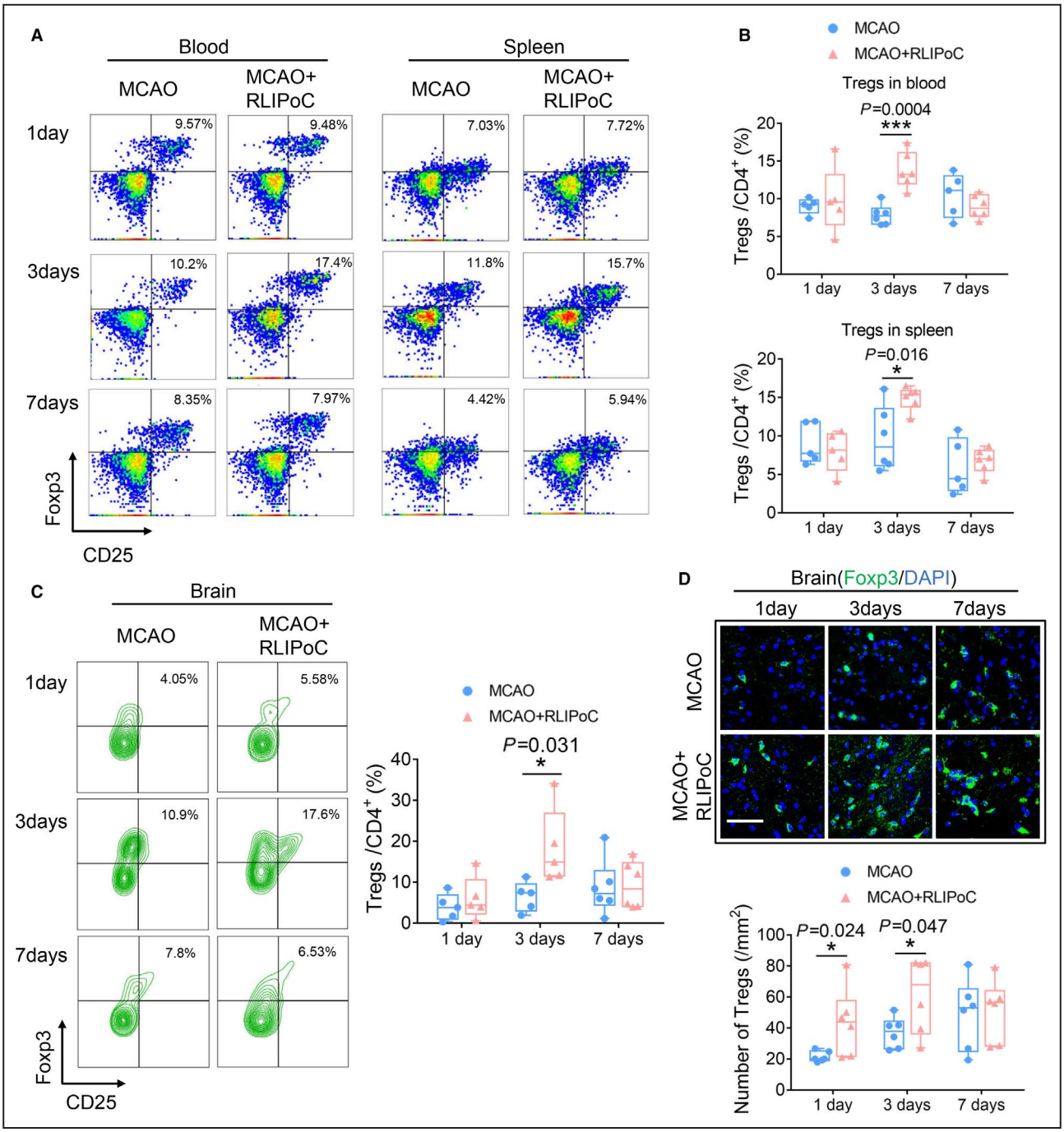

Figure 2. RLIPoC increases Tregs abundance in the blood, spleen, and brain.
A, Representative flow cytometry plots of $CD4^+$ $CD25^+$ $Foxp3^+$ Tregs in the blood and spleen on day 1, 3, and 7 after MCAO. **B**, Quantification of percentages of $CD25^+$ $Foxp3^+$ Tregs among $CD4^+$ T cells in the blood and spleen. Student *t* test, $^*P<0.05$, $^{***}P<0.001$ vs MCAO. n=5 to 6 per group. **C**, Representative flow cytometry plots and quantification of percentages of $CD25^+$ $Foxp3^+$ Tregs among $CD4^+$ T cells in ipsilateral hemispheres on days 1, 3, and 7 after MCAO were shown in the histogram. Student *t* test, $^*P<0.05$ vs MCAO. n=5 to 6 per group. **D**, Tregs number at peri-infarct area was evaluated using transgenic mice with EGFP-tagged Foxp3 at different time points after MCAO. Representative confocal images of coronal sections labeled Tregs with EGFP and quantification of EGFP-positive cells are shown in the histogram. Scale bar=50 μm. Student *t* test, $^*P<0.05$ vs MCAO. n=6 per group. EGFP indicates enhanced green fluorescence protein; MCAO, middle cerebral artery occlusion; RLIPoC, remote limb ischemic postconditioning; and Tregs, regulatory T cells.

we then investigated whether RLIPoC-induced neuroprotection was mediated by Tregs after MCAO. $CD4^+CD25^+$ Tregs were magnetically isolated from donor mice with a degree of purity as high as 93.3% (Figure S3), and were then transferred into recipient mice (intravenous, 1×10^6/mouse) within 1 hour after

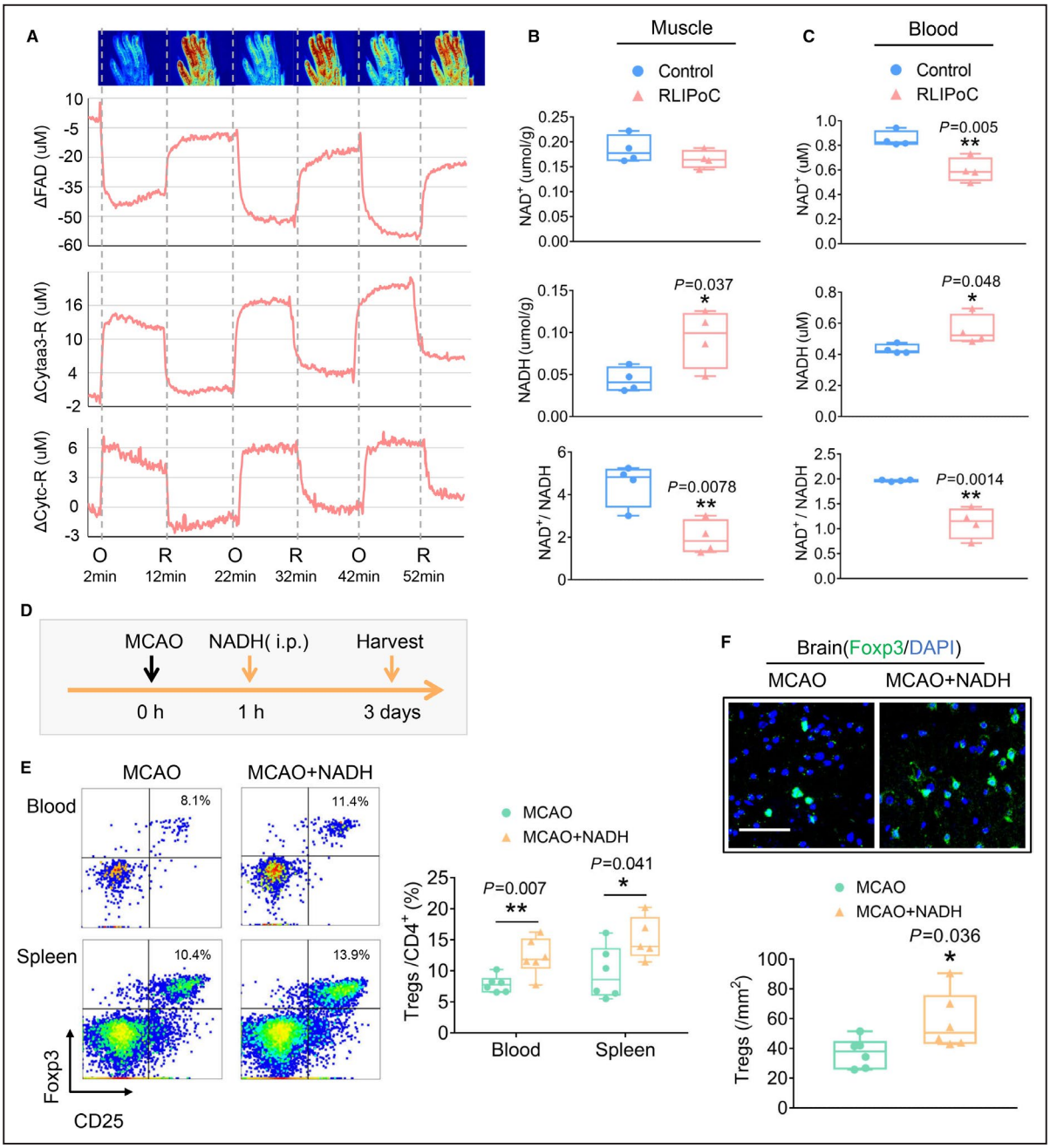

Figure 3. RLIPoC facilitated Tregs increase via modifying metabolic spectrum.
A, Images of blood flow (top) and curves of the dynamic concentration changes of metabolites (FAD, Cytaa3-R, and Cytc-R) in the region of the hind limb underwent RLIPoC in vivo, which was monitored using a multispectral optical imaging system. O indicates occlusion of the bilateral femoral arteries; and R, reperfusion of the bilateral femoral arteries. **B**, Concentrations of NAD^+ and NADH, and the ratio of NAD^+ to NADH, in muscle that underwent RLIPoC. Student *t* test, $^*P<0.05$, $^{**}P<0.01$ vs control. n=4 per group. **C**, Concentrations of NAD^+ and NADH and the ratio of NAD^+ to NADH in the blood. Student *t* test, $^*P<0.05$, $^{**}P<0.01$ vs control. n=4 per group. **D**, Scheme for NADH administration. NADH (intraperitoneal 50 mg/mouse) was administered within 1 hour after the MCAO model, and the mouse was euthanized at 3 days after MCAO and NADH administration. **E**, Representative flow cytometry plots and quantitation of percentages of $CD25^+$ $Foxp3^+$ Tregs among $CD4^+$ T cells in the blood and spleen after 3 days of MCAO are shown in the histogram. Student *t* test, $^*P<0.05$, $^{**}P<0.01$ vs MCAO. n=5 to 6 per group. **F**, Representative confocal images of coronal sections labeled Tregs with EGFP, and quantification of EGFP-positive cells are shown in the histogram. Scale bar=50 μm. Student *t* test, $^*P<0.05$ vs MCAO. n=6 per group. Cytaa3-R indicates cytochrome aa3 in a reduced state; Cytc-R, cytochrome c in a reduced state; EGFP, enhanced green fluorescence protein; FAD, flavin adenine dinucleotide; MCAO, middle cerebral artery occlusion; NAD+, nicotinamide adenine dinucleotide; NADH, nicotinamide adenine dinucleotide hydrate; RLIPoC, remote limb ischemic postconditioning; and Tregs, regulatory T cells.

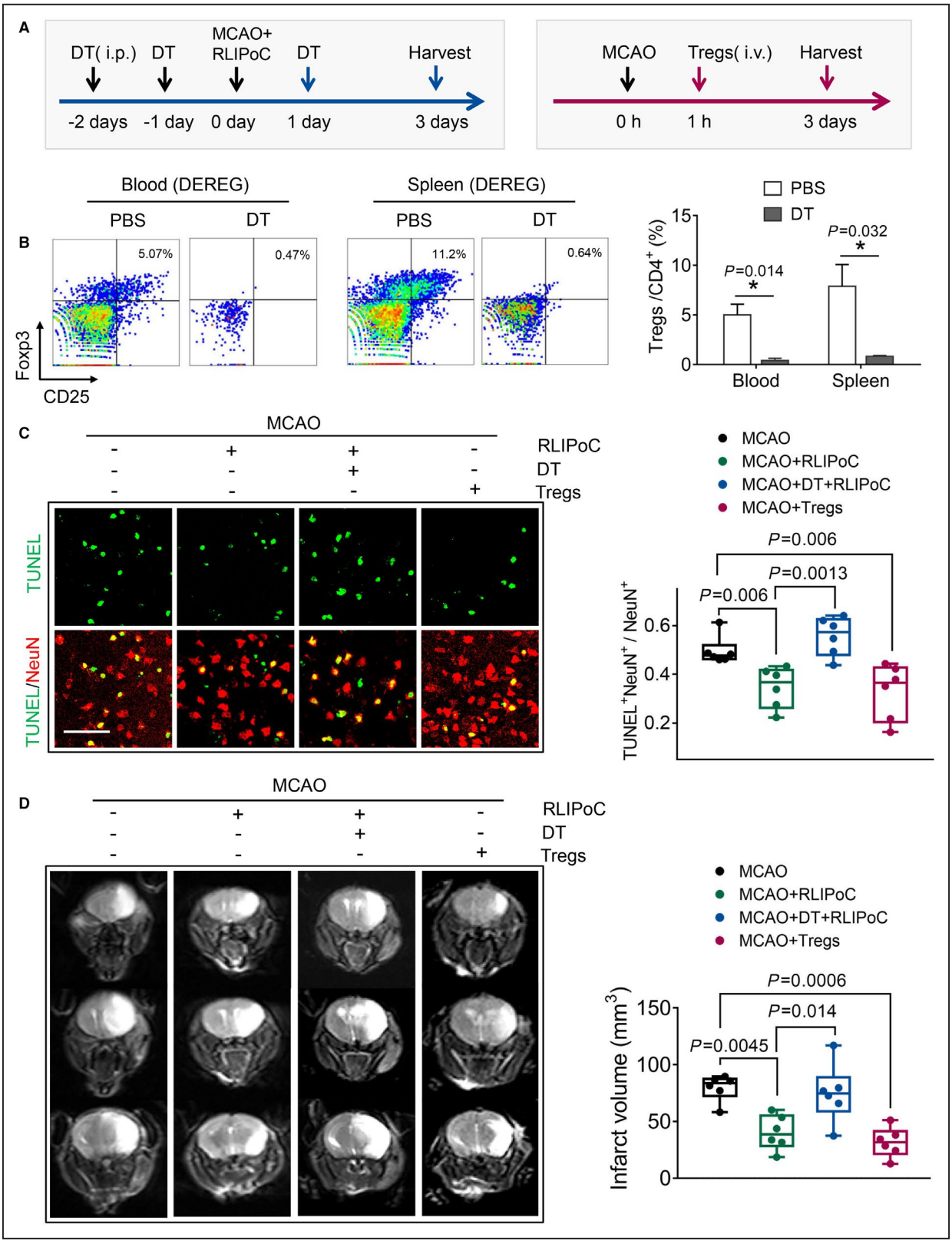

MCAO, named the MCAO+Tregs group (Figure 4A). We also conditionally depleted endogenous Tregs in DEREG mice via injection of DT (Figure 4A). The efficacy of ablation was confirmed by flow cytometry in the blood and spleen, and more than 90% Tregs were successfully depleted (Figure 4B). TUNEL staining was performed to evaluate neuronal apoptosis at the peri-infarct region. Tregs injection or RLIPoC treatment

Figure 4. Depletion of Tregs in vivo abolished neuroprotection conferred by RLIPoC.
A, Scheme for ablation of Tregs in DEREG mice (left) and purified Tregs transferring to recipient mice (right). Diphtheria toxin (DT; intraperitoneal, 50 μg/kg body weight) was administered 2 days before the MCAO model and was administered again with a dose of 10 μg/kg body weight every other day until the mouse was euthanized. Purified $CD4^+CD25^+$ Tregs were transferred intravenously to recipient mice within 1 hour after the MCAO model, with a dose of 1 million per mouse through the tail vein. **B**, The efficacy of Tregs ablation in DEREG mice using DT. Representative flow cytometry plots and the quantitation of percentages of $CD25^+$ $Foxp3^+$ Tregs among $CD4^+$ T cells in the blood and spleen are shown in the histogram. Student *t* test, $^*P<0.05$ vs PBS. n=3 per group. **C**, Neuronal apoptosis was assessed by TUNEL staining at 3 days after MCAO. Representative confocal images of coronal sections labeled with TUNEL and NeuN; the quantitation of NeuN and TUNEL double positive cells are shown in the histogram. Scale bar=50 μm. Kruskal-Wallis test with Dunn's post hoc test. n=6 per group. **D**, Representative magnetic resonance images and quantification of infarct volume at 3 days after MCAO. One-way ANOVA with Bonferroni's post hoc test. n=6 per group. DEREG indicates depletion of regulatory T cell; MCAO, middle cerebral artery occlusion; NeuN, neuronal nuclei; RLIPoC, remote limb ischemic postconditioning; Tregs, regulatory T cells; and TUNEL, terminal deoxynucleotidal transferase–mediated biotin–deoxyuridine triphosphate nick-end labeling.

significantly attenuated brain injury with the reduction of neuronal apoptosis percentage, compared with the MCAO group (Figure 4C), on day 3 after MCAO. Of note, RLIPoC-mediated neuronal protection was blockaded in Tregs-depleted DEREG mice (Figure 4C). In addition, we assessed the infarct volume by performing magnetic resonance imaging. The results showed that RLIPoC treatment resulted in a smaller infract volume, but the depletion of Tregs abolished the RLIPoC-mediated decrease of infarct volume (Figure 4D).

Collectively, these results suggested that RLIPoC-induced neuroprotection through increasing Tregs, and conditional depletion of Tregs abrogated RLIPoC-mediated neuroprotection after MCAO.

Microglia/Macrophages Were a Major Target for the Anti-Inflammatory/Neuroprotective Effect of Tregs

As the resident immunocyte in the central nervous system, microglia play a prominent role in orchestrating the inflammatory response to ischemic stroke.[43] $Iba\text{-}1^+$ microglia/macrophages were observed in close proximity to EGFP-tagged Tregs in the peri-infarct area (Figure S4). To investigate the influence of RLIPoC or Tregs on microglia/macrophages, we evaluated several pro/anti-inflammatory markers expressed in microglia/macrophages surrounding the infarct at 3 days after MCAO using immunofluorescent staining. The border of infarct was defined by the accumulation and morphology of $Iba\text{-}1^+$ cells (Figure S5), and $Iba\text{-}1^+$ microglia/macrophages at the border of infarct were captured and analyzed. CD16/32 and major histocompatibility complex II, proinflammatory markers expressed in microglia/macrophages, were significantly decreased after RLIPoC treatment or Tregs injection, whereas Tregs depletion abrogated this effect mediated by RLIPoC treatment (Figure 5A and 5B). Unexpectedly, RLIPoC/Tregs treatment did not facilitate microglia/macrophages phenotyping toward an anti-inflammatory profile, as anti-inflammatory markers (CD206 and Arg-1) did not show significant changes (Figure 5C and 5D).

Remote ischemic postconditioning influences the inflammatory status via various aspects.[44] To investigate the effects of Tregs on microglia directly, we carried out oxygen-glucose deprivation (OGD) to mimic ischemic conditions in vitro. Tregs magnetically enriched from splenocytes were cocultured with primary microglia that suffered from OGD. Immunofluorescent staining revealed that Tregs administration resulted in a decrease of proinflammatory markers (CD16/32) (Figure 6A through 6C). Reverse transcription-polymerase chain reaction was performed to evaluate much more proinflammatory markers, and results showed that Tregs-cocultured microglia were associated with substantially lower expression of proinflammatory genes (Figure 6D). Finally, we also evaluated microglia phagocytosis using fluorescent particles (Zymosan A BioParticles conjugated with Alexa Fluor 488) and found that Tregs decreased the number of particles phagocytized by microglia (Figure 6E). Consistent with the results from the phagocytosis assay, reverse transcription-polymerase chain reaction further confirmed that Tregs attenuated phagocytosis-related gene expression in microglia (Figure 6F).

Taken together, these results indicate that Tregs partially exhibit neuroprotective effects via inhibiting inflammation and phagocytosis of microglia/macrophages.

DISCUSSION

Ischemic postconditioning, an emerging therapeutic approach of ischemic stroke that targets multiple pathways involved in ischemic injury, has proven to be promising.[44,45] However, the underlying mechanism of its neuroprotective effects needs further elucidation. In the present study, we found that (1) RLIPoC reduces neuronal apoptosis and improves neurological outcomes after ischemic stroke; (2) these neuroprotective effects might result from the increased peripheral Tregs count and brain Tregs infiltration after RLIPoC; (3) RLIPoC induces the increase of Tregs via modulation of metabolites, including FAD and NAD^+/NADH; and (4) RLIPoC attenuates neuroinflammation in ischemic lesions by the anti-inflammatory action of Tregs toward active microglia/macrophages (Figure 7). Remote ischemic postconditioning, easily feasible in patients, was demonstrated to be neuroprotective

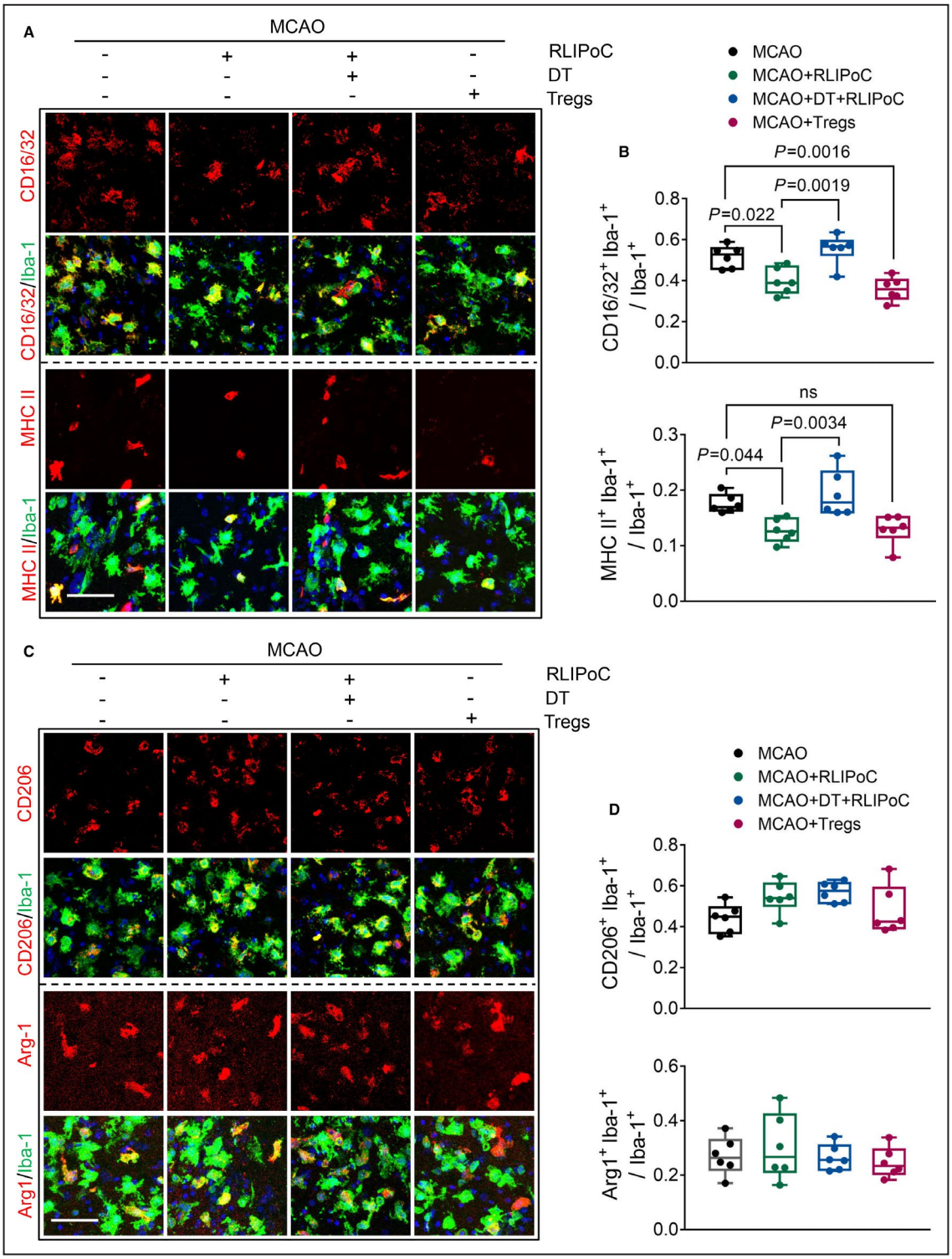

Figure 5. Tregs attenuated proinflammation of microglia/macrophages in vivo.
A, Representative confocal images of coronal sections labeled with Iba-1, CD16/32, and MHC II at 3 days after MCAO. Scale bar=50 μm. **B**, Quantitative analysis of Iba-1, CD16/32 double positive cells and Iba-1, MHC II double positive cells, at 3 days after MCAO. One-way ANOVA with Bonferroni's post hoc test. n=6 per group. ns, not significant. **C**, Representative confocal images of coronal sections labeled with Iba-1, CD206, and Arg-1 at 3 days after MCAO. Scale bar=50 μm. **D**, Quantitative analysis of Iba-1, CD206 double positive cells and Iba-1, Arg-1 double positive cells, at 3 days after MCAO. One-way ANOVA with Bonferroni's post hoc test. n=6 per group. DT indicates diphtheria toxin; MCAO, middle cerebral artery occlusion; MHC II, major histocompatibility complex II; RLIPoC, remote limb ischemic postconditioning; and Tregs, regulatory T cells.

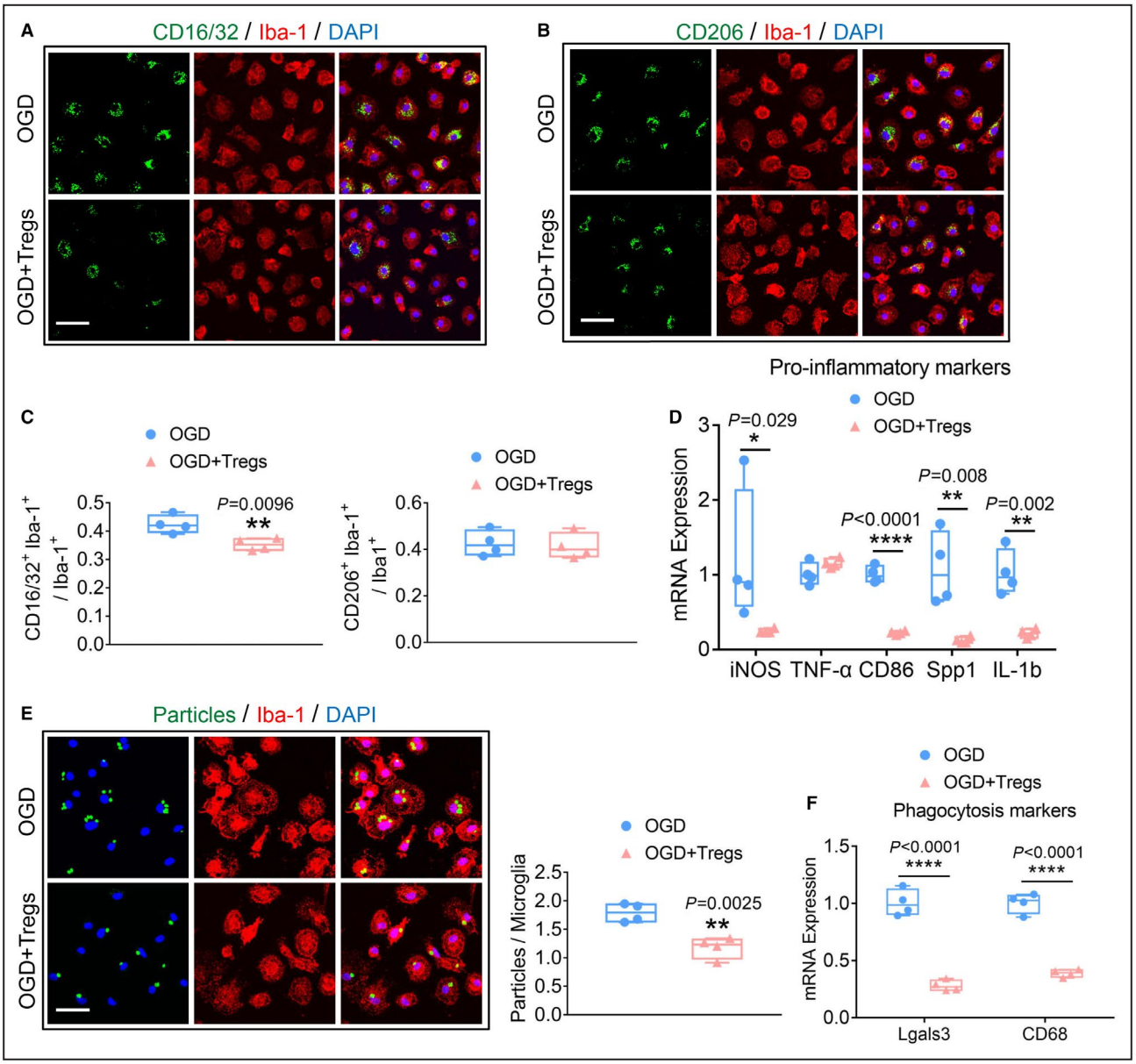

Figure 6. Tregs attenuated proinflammation and phagocytosis of microglia in vitro.
Representative confocal images of primary cultured microglia labeled with Iba-1, CD16/32 (**A**) and CD206 (**B**) 4 hours after OGD, with subsequent 24-hour reoxidation. Scale bar=50 μm. **C**, Quantitative analysis of Iba-1, CD16/32 double positive cells and Iba-1, CD206 double positive cells, 4 hours after OGD with subsequent 24-hour re-oxidation. Student *t* test, ***P*<0.01 vs OGD. n=4 per group. **D**, The mRNA expression of pro-inflammatory markers (iNOS, TNF-α, CD86, Spp1, and IL-1β) in primary cultured microglia was detected by quantitative real-time PCR, after OGD 4 hours with subsequent 24-hours reoxidation. Student *t* test (the mRNA expression of iNOS was assessed by Mann-Whitney test), **P*<0.05 vs OGD, ***P*<0.01, *****P*<0.0001 vs OGD. n=4 per group. **E**, Representative confocal images of primary cultured microglia labeled with Iba-1, Zymosan A BioParticles conjugated with Alexa Fluor 488 (Particles), and the quantitative analysis of the number of particles phagocytized by microglia, 4 hours after OGD with subsequent 24-hour reoxidation. Scale bar=50 μm. Student *t* test, ***P*<0.01 vs OGD. n=4 per group. **F**, The mRNA expression of phagocytosis markers (CD68 and Lgals3) in primary cultured microglia was detected by quantitative real-time PCR, 4 hours after OGD with subsequent 24-hour re-oxidation. Student *t* test, *****P*<0.0001 vs OGD. n=4 per group. IL indicates interleukin; iNOS, inducible nitric oxide synthase; OGD, oxygen-glucose deprivation; PCR, polymerase chain reaction; Spp1, secreted phosphoprotein 1; TNF-α, tumor necrosis factor-alpha; and Tregs, regulatory T cells.

against ischemic stroke.[44,45] Immunocytes were involved in the process of remote ischemic conditioning. Neutrophil adhesion and phagocytosis were significantly decreased after remote forearm ischemic preconditioning.[13] Interestingly, T lymphocytes also proved to be susceptible to remote ischemic post/preconditioning.[33,46] Remote ischemic preconditioning can elevate the percentage of $CD3^+CD8^+$ cytotoxic

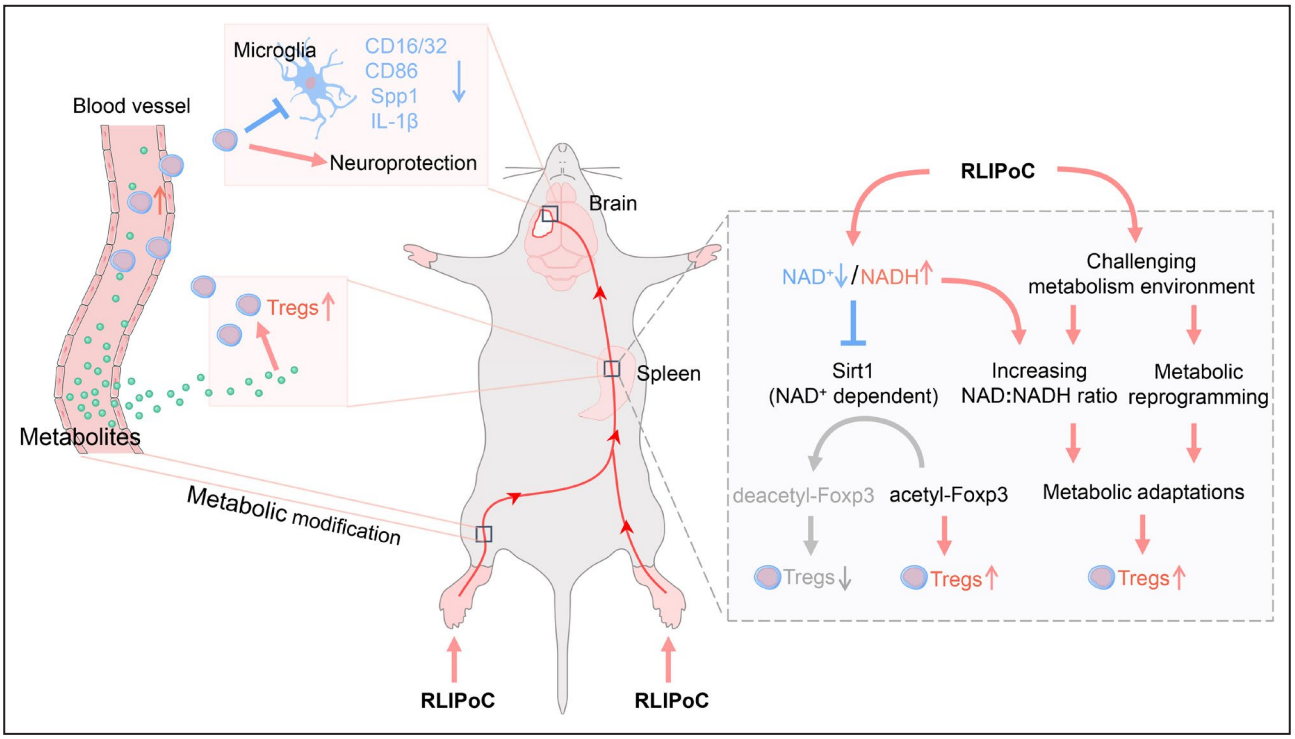

Figure 7. Schematic illustration of the mechanisms for RLIPoC-induced upregulation of Tregs with subsequent neuroprotection in ischemic stroke.

RLIPoC is accompanied by metabolic modification and concentration changes of some metabolites. NAD^+:NADH ratio decrease leads to Sirt1 (Sirtuin-1) inhibition followed by upregulation of Foxp3 acetylation, which promotes the production of $Foxp3^+$ Tregs.[41] In addition, Tregs have metabolic advantages of enhancing the NAD^+:NADH ratio and metabolic reprogramming, these metabolic adaptations allowing Tregs to thrive in challenging metabolism milieu.[35,36] Tregs attenuate neuroinflammation by suppressing microglia polarization to a proinflammatory response and ultimately protect against brain injury in ischemic stroke. IL indicates interleukin; NAD+, nicotinamide adenine dinucleotide; NADH, nicotinamide adenine dinucleotide hydrate; RLIPoC, remote limb ischemic postconditioning; and Tregs, regulatory T cells.

cells in the spleen; in contrast, it resulted in a reduction of circulating cytotoxic T cells.[46] The percentage of $CD4^+$ T cells in the spleen and $CD8^+$ T cells in the blood were found to be increased after RLIPoC.[33] Besides, metal responsive transcription factor, association with Tregs function, could be triggered by RLIPoC.[47] All of these findings suggested that T lymphocytes are susceptible to remote ischemic conditioning. Meanwhile, it was increasingly elucidated that adaptive immunity is also involved in the pathological process of ischemic stroke inflammation, as well as innate immunocytes, such as microglia or macrophages and neutrophils.[14] In this study, we observed significant increases of Tregs abundancy in the spleen, blood, and brain tissue surrounding infarct lesions 3 days after MCAO with RLIPoC treatment. As a specific subset of T lymphocytes, Tregs can attenuate inflammation in ischemic stroke without aggravation of poststroke immunosuppression, which could increase the risk of infection after ischemic stroke.[16,18,48] As the neuroprotective effects of RLIPoC were abolished in DEREG mice, we demonstrated that RLIPoC-mediated neuroprotection against ischemic stroke was at least partially attributed to the upregulation of Tregs. However, the neuroprotective effects from remote ischemic postconditioning and the underlying mechanisms in RLIPoC-induced upregulation of Tregs remains unclear.

Humoral factors, such as adenosine and bradykinin, and some neurogenic factors have been reported to be involved in the mechanisms underlying cross-organ protection mediated by remote ischemic conditioning.[44,45,49] Intriguingly, similar to plasma from donor rabbits that induced remote ischemic preconditioning, the dialysate of plasma obtained using a 15-kDa cut-off dialysis membrane could also protect the isolated heart against infarction.[50] This finding indicated that some low molecular mass (<15 kDa) circulating factors might also be involved in the neuroprotection of remote ischemic conditioning. Presumably, metabolites, often with low molecular mass, might be the circulating mediators transferring the protective effects. Therefore, we determined the dynamic changes of metabolites during RLIPoC, which have not been studied before, using a multispectral optical imaging system.[25] As expected, the relative levels of FAD, Cytaa3-R, and Cytc-R in RLIPoC-conducted limbs substantially fluctuated with episodes of ischemia/reperfusion

conditioning, and FAD was significantly decreased in ischemia, which was consistent with previous studies.[39] In contrast with FAD, NADH was elevated after RLIPoC, both in limb muscle tissues (RLIPoC-conducted limbs) and circulating plasma. NAD^+/NADH and the NAD^+:NADH ratio, have been demonstrated to be related with the function and proliferation/apoptosis of Tregs.[35,40,41,51] $CD4^+$ T cell subsets have distinct metabolic features.[34] Different from $CD4^+$ effector T cells, Tregs are more tolerable to the ischemic milieu. In the condition of NAD^+:NADH ratio decrease, Tregs transcription factor Foxp3 modifies cell metabolism and results in elevating NAD^+ regeneration.[35] The decline of NAD^+ suppresses the activity of Sirtuin-1, a type of deacetylase dependent on NAD^+, which enhances Foxp3 acetylation and ultimately favors the thriving of Tregs.[41] Our data suggested that RLIPoC modified the spectrum of metabolites and especially decreased the NAD^+:NADH ratio both in RLIPoC-conducted local tissues and circulating blood, through which metabolites could be transferred into the brain and spleen. These metabolites' changes might enhance the production of Tregs in the spleen and lymph nodes, followed by a subsequent release into the blood and infiltration into the brain. In addition, this increase of Tregs abundance both in the blood and brain could be simulated by reducing the NAD^+:NADH ratio with administration of NADH.

Tregs could attenuate inflammation after ischemic stroke in diverse pathways. Tregs transplantation could inhibit the MMP9 (matrix metallopeptidase-9) production in blood neutrophils and decrease the number $MMP9^+$ neutrophils infiltrating into the brain.[18] Secretion of interleukin-10 from Tregs could decrease TNF-α production from microglia at 24 hours after MCAO and mitigate interferon γ production in brain-infiltrating T cells at 5 days after MCAO.[16] Tregs expressed interleukin-4 in mice with amyotrophic lateral sclerosis, which augmented protective M2 microglia.[52] Tregs could also increase the reparative activity of microglia via section of osteopontin in ischemic stroke, thereby alleviating brain injury.[53] Besides, microglia was demonstrated to suppress T cell proliferation in mice with experimental autoimmune encephalomyelitis.[54] Overall, there was comprehensive cross-talk between Tregs and microglia in brain. Of note, our results revealed that the anti-inflammatory effect of RLIPoC was mediated by Tregs infiltration into the ischemic brain, and Tregs could prevent microglia/macrophages exhibiting a proinflammatory profile rather than upregulating the expression of anti-inflammatory genes, which was a possible underlying neuroprotective mechanism of RLIPoC.

CONCLUSIONS

In conclusion, our study revealed that Tregs was involved in the neuroprotection of RLIPoC against ischemic stroke. Depletion of Tregs using DEREG mice abolished the neuroprotection induced by RLIPoC. Accompanied by subsequent metabolite-spectrum alteration following RLIPoC, Tregs were more preferable to the metabolically challenging milieu, especially the decreasing ratio of NAD^+:NADH, which facilitated the thriving of Tregs in the peri-infarct region after ischemic stroke. Finally, Tregs attenuated neuroinflammation via suppressing the microglia/macrophages proinflammatory profile surrounding the ischemic lesions. Our research elucidated a novel neuroprotective mechanism underlying remote ischemic postconditioning.

ARTICLE INFORMATION

Received July 9, 2021; accepted September 13, 2021.

Affiliations

Department of Neurology, Tongji Hospital, Tongji Medical College, Huazhong University of Science and Technology, Wuhan, China (H.-H.Y., X.-T.M., X.M., M.C., Y.-H.C., W.W., C.Q., D.-S.T.); Department of Neurology, Shandong Provincial Hospital, Shandong First Medical University, Jinan, China (X.-T.M.); and Department of Neurology, Mayo Clinic, Rochester, MN MN (L.-J.W.).

Sources of Funding

This work was supported by the National Natural Science Foundation of China (Grants: 82071380, 81873743, 81801223) and the Tongji Hospital (HUST) Foundation for Excellent Young Scientist (Grant No. 2020YQ06).

Disclosures

None.

Supplementary Material

Figures S1–S5

REFERENCES

1. Feigin VL, Lawes CM, Bennett DA, Barker-Collo SL, Parag V. Worldwide stroke incidence and early case fatality reported in 56 population-based studies: a systematic review. *Lancet Neurol*. 2009;8:355–369. doi: 10.1016/S1474-4422(09)70025-0
2. Wang W, Jiang B, Sun H, Ru X, Sun D, Wang L, Wang L, Jiang Y, Li Y, Wang Y, et al. Prevalence, incidence, and mortality of stroke in china: results from a nationwide population-based survey of 480 687 adults. *Circulation*. 2017;135:759–771. doi: 10.1161/CIRCULATIONAHA.116.025250
3. Hacke W, Kaste M, Bluhmki E, Brozman M, Dávalos A, Guidetti D, Larrue V, Lees KR, Medeghri Z, Machnig T, et al. Thrombolysis with alteplase 3 to 4.5 hours after acute ischemic stroke. *N Engl J Med*. 2008;359:1317–1329. doi: 10.1056/NEJMoa0804656
4. Sandercock P, Wardlaw JM, Lindley RI, Dennis M, Cohen G, Murray G, Innes K, Venables G, Czlonkowska A, Kobayashi A, et al. The benefits and harms of intravenous thrombolysis with recombinant tissue plasminogen activator within 6 h of acute ischaemic stroke (the third international stroke trial [IST-3]): a randomised controlled trial. *Lancet*. 2012;379:2352–2363. doi: 10.1016/s0140-6736(12)60768-5
5. Wardlaw JM, Murray V, Berge E, del Zoppo G, Sandercock P, Lindley RL, Cohen G. Recombinant tissue plasminogen activator for acute ischaemic stroke: an updated systematic review and meta-analysis. *Lancet*. 2012;379:2364–2372. doi: 10.1016/S0140-6736(12)60738-7
6. Zhao ZQ, Corvera JS, Halkos ME, Kerendi F, Wang NP, Guyton RA, Vinten-Johansen J. Inhibition of myocardial injury by ischemic postconditioning during reperfusion: comparison with ischemic preconditioning. *Am J Physiol Heart Circ Physiol*. 2003;285:H579–H588. doi: 10.1152/ajpheart.01064.2002
7. Kerendi F, Kin H, Halkos ME, Jiang R, Zatta AJ, Zhao ZQ, Guyton RA, Vinten-Johansen J. Remote postconditioning. Brief renal ischemia

and reperfusion applied before coronary artery reperfusion reduces myocardial infarct size via endogenous activation of adenosine receptors. *Basic Res Cardiol*. 2005;100:404–412. doi: 10.1007/s00395-005-0539-2
8. Gao X, Ren C, Zhao H. Protective effects of ischemic postconditioning compared with gradual reperfusion or preconditioning. *J Neurosci Res*. 2008;86:2505–2511. doi: 10.1002/jnr.21703
9. Li C-Y, Ma W, Liu K-P, Yang J-W, Wang X-B, Wu Z, Zhang T, Wang J-W, Liu W, Liu J, et al. Advances in intervention methods and brain protection mechanisms of in situ and remote ischemic postconditioning. *Metab Brain Dis*. 2021;36:53–65. doi: 10.1007/s11011-020-00562-x
10. Shu Y, Li Z, Han B. Penehyclidine hydrochloride postconditioning ameliorates cerebral ischemia-reperfusion injury: critical role of mitochondrial atp sensitive potassium channel. *J Biol Regul Homeost Agents*. 2016;30:41–53.
11. Xing B, Chen H, Zhang M, Zhao D, Jiang R, Liu X, Zhang S. Ischemic postconditioning inhibits apoptosis after focal cerebral ischemia/reperfusion injury in the rat. *Stroke*. 2008;39:2362–2369. doi: 10.1161/STROKEAHA.107.507939
12. Kong Y, Rogers MR, Qin X. Effective neuroprotection by ischemic postconditioning is associated with a decreased expression of RGMa and inflammation mediators in ischemic rats. *Neurochem Res*. 2013;38:815–825. doi: 10.1007/s11064-013-0984-5
13. Shimizu M, Saxena P, Konstantinov IE, Cherepanov V, Cheung MM, Wearden P, Zhangdong H, Schmidt M, Downey GP, Redington AN. Remote ischemic preconditioning decreases adhesion and selectively modifies functional responses of human neutrophils. *J Surg Res*. 2010;158:155–161. doi: 10.1016/j.jss.2008.08.010
14. Machhi J, Kevadiya BD, Muhammad IK, Herskovitz J, Olson KE, Mosley RL, Gendelman HE. Harnessing regulatory T cell neuroprotective activities for treatment of neurodegenerative disorders. *Mol Neurodegener*. 2020;15:32. doi: 10.1186/s13024-020-00375-7
15. McGeachy MJ, Stephens LA, Anderton SM. Natural recovery and protection from autoimmune encephalomyelitis: contribution of $CD4^+CD25^+$ regulatory cells within the central nervous system. *J Immunol*. 2005;175:3025–3032.
16. Liesz A, Suri-Payer E, Veltkamp C, Doerr H, Sommer C, Rivest S, Giese T, Veltkamp R. Regulatory T cells are key cerebroprotective immunomodulators in acute experimental stroke. *Nat Med*. 2009;15:192–199. doi: 10.1038/nm.1927
17. Vignali DA, Collison LW, Workman CJ. How regulatory T cells work. *Nat Rev Immunol*. 2008;8:523–532. doi: 10.1038/nri2343
18. Li P, Gan Y, Sun BL, Zhang F, Lu B, Gao Y, Liang W, Thomson AW, Chen J, Hu X. Adoptive regulatory T-cell therapy protects against cerebral ischemia. *Ann Neurol*. 2013;74:458–471. doi: 10.1002/ana.23815
19. Ito M, Komai K, Mise-Omata S, Iizuka-Koga M, Noguchi Y, Kondo T, Sakai R, Matsuo K, Nakayama T, Yoshie O, et al. Brain regulatory T cells suppress astrogliosis and potentiate neurological recovery. *Nature*. 2019;565:246–250. doi: 10.1038/s41586-018-0824-5
20. Offner H, Subramanian S, Parker SM, Wang C, Afentoulis ME, Lewis A, Vandenbark AA, Hurn PD. Splenic atrophy in experimental stroke is accompanied by increased regulatory T cells and circulating macrophages. *J Immunol*. 2006;176:6523–6531. doi: 10.4049/jimmunol.176.11.6523
21. Yan J, Greer JM, Etherington K, Cadigan GP, Cavanagh H, Henderson RD, O'Sullivan JD, Pandian JD, Read SJ, McCombe PA. Immune activation in the peripheral blood of patients with acute ischemic stroke. *J Neuroimmunol*. 2009;206:112–117. doi: 10.1016/j.jneuroim.2008.11.001
22. Kleinschnitz C, Kraft P, Dreykluft A, Hagedorn I, Göbel K, Schuhmann MK, Langhauser F, Helluy X, Schwarz T, Bittner S, et al. Regulatory T cells are strong promoters of acute ischemic stroke in mice by inducing dysfunction of the cerebral microvasculature. *Blood*. 2013;121:679–691. doi: 10.1182/blood-2012-04-426734
23. Huo W, Liu Y, Lei Y, Zhang Y, Huang Y, Mao Y, Wang C, Sun Y, Zhang W, Ma Z, et al. Imbalanced spinal infiltration of Th17/Treg cells contributes to bone cancer pain via promoting microglial activation. *Brain Behav Immun*. 2019;79:139–151. doi: 10.1016/j.bbi.2019.01.024
24. Belayev L, Busto R, Zhao W, Fernandez G, Ginsberg MD. Middle cerebral artery occlusion in the mouse by intraluminal suture coated with poly-L-lysine: neurological and histological validation. *Brain Res*. 1999;833:181–190. doi: 10.1016/S0006-8993(99)01528-0
25. Yin C, Zhou F, Wang Y, Luo W, Luo Q, Li P. Simultaneous detection of hemodynamics, mitochondrial metabolism and light scattering changes during cortical spreading depression in rats based on multi-spectral optical imaging. *Neuroimage*. 2013;76:70–80. doi: 10.1016/j.neuroimage.2013.02.079
26. Mock JR, Garibaldi BT, Aggarwal NR, Jenkins J, Limjunyawong N, Singer BD, Chau E, Rabold R, Files DC, Sidhaye V, et al. Foxp3+ regulatory T cells promote lung epithelial proliferation. *Mucosal Immunol*. 2014;7:1440–1451. doi: 10.1038/mi.2014.33
27. Hu Z-W, Zhou L-Q, Yang S, Chen M, Yu H-H, Tao R, Wu L-J, Wang W, Zhang Q, Qin C, et al. FTY720 modulates microglia toward anti-inflammatory phenotype by suppressing autophagy via STAT1 pathway. *Cell Mol Neurobiol*. 2021;41:353–364. doi: 10.1007/s10571-020-00856-9
28. Qin C, Liu Q, Hu ZW, Zhou LQ, Shang K, Bosco DB, Wu LJ, Tian DS, Wang W. Microglial TLR4-dependent autophagy induces ischemic white matter damage via STAT1/6 pathway. *Theranostics*. 2018;8:5434–5451.
29. Chen J, Li Y, Wang L, Zhang Z, Lu D, Lu M, Chopp M. Therapeutic benefit of intravenous administration of bone marrow stromal cells after cerebral ischemia in rats. *Stroke*. 2001;32:1005–1011. doi: 10.1161/01.STR.32.4.1005
30. Zhou Y, Fathali N, Lekic T, Ostrowski RP, Chen C, Martin RD, Tang J, Zhang JH. Remote limb ischemic postconditioning protects against neonatal hypoxic-ischemic brain injury in rat pups by the opioid receptor/Akt pathway. *Stroke*. 2011;42:439–444. doi: 10.1161/STROKEAHA.110.592162
31. Zhang W, Miao Y, Zhou S, Jiang J, Luo Q, Qiu Y. Neuroprotective effects of ischemic postconditioning on global brain ischemia in rats through upregulation of hippocampal glutamine synthetase. *J Clin Neurosci*. 2011;18:685–689. doi: 10.1016/j.jocn.2010.08.027
32. Konstantinov IE, Arab S, Kharbanda RK, Li J, Cheung MMH, Cherepanov V, Downey GP, Liu PP, Cukerman E, Coles JG, et al. The remote ischemic preconditioning stimulus modifies inflammatory gene expression in humans. *Physiol Genomics*. 2004;19:143–150. doi: 10.1152/physiolgenomics.00046.2004
33. Liu C, Yang J, Zhang C, Geng X, Zhao H. The changes of systemic immune responses during the neuroprotection induced by remote ischemic postconditioning against focal cerebral ischemia in mice. *Neurol Res*. 2019;41:26–36. doi: 10.1080/01616412.2018.1523037
34. Gerriets VA, Kishton RJ, Nichols AG, Macintyre AN, Inoue M, Ilkayeva O, Winter PS, Liu X, Priyadharshini B, Slawinska ME, et al. Metabolic programming and PDHK1 control $CD4^+$ T cell subsets and inflammation. *J Clin Invest*. 2015;125:194–207. doi: 10.1172/JCI76012
35. Angelin A, Gil-de-Gómez L, Dahiya S, Jiao J, Guo L, Levine MH, Wang Z, Quinn WJ III, Kopinski PK, Wang L, et al. Foxp3 reprograms T cell metabolism to function in low-glucose, high-lactate environments. *Cell Metab*. 2017;25:1282–1293.e1287. doi: 10.1016/j.cmet.2016.12.018
36. Pacella I, Procaccini C, Focaccetti C, Miacci S, Timperi E, Faicchia D, Severa M, Rizzo F, Coccia EM, Bonacina F, et al. Fatty acid metabolism complements glycolysis in the selective regulatory T cell expansion during tumor growth. *Proc Natl Acad Sci USA*. 2018;115:E6546–E6555. doi: 10.1073/pnas.1720113115
37. Macintyre AN, Gerriets VA, Nichols AG, Michalek RD, Rudolph MC, Deoliveira D, Anderson SM, Abel ED, Chen BJ, Hale LP, et al. The glucose transporter Glut1 is selectively essential for CD4 T cell activation and effector function. *Cell Metab*. 2014;20:61–72.
38. Ghesquière B, Wong BW, Kuchnio A, Carmeliet P. Metabolism of stromal and immune cells in health and disease. *Nature*. 2014;511:167–176. doi: 10.1038/nature13312
39. Papayan G, Petrishchev N, Galagudza M. Autofluorescence spectroscopy for NADH and flavoproteins redox state monitoring in the isolated rat heart subjected to ischemia-reperfusion. *Photodiagnosis Photodyn Ther*. 2014;11:400–408. doi: 10.1016/j.pdpdt.2014.05.003
40. Nation CS, Da'Dara AA, Skelly PJ. The essential schistosome tegumental ectoenzyme SmNPP5 can block NAD-induced T cell apoptosis. *Virulence*. 2020;11:568–579. doi: 10.1080/21505594.2020.1770481
41. Chadha S, Wang L, Hancock WW, Beier UH. Sirtuin-1 in immunotherapy: a Janus-headed target. *J Leukoc Biol*. 2019;106:337–343. doi: 10.1002/JLB.2RU1118-422R
42. Zhang H, Xia Y, Ye Q, Yu F, Zhu W, Li P, Wei Z, Yang Y, Shi Y, Thomson AW, et al. In vivo expansion of regulatory T cells with IL-2/IL-2 antibody complex protects against transient ischemic stroke. *J Neurosci*. 2018;38:10168–10179.
43. Jayaraj RL, Azimullah S, Beiram R, Jalal FY, Rosenberg GA. Neuroinflammation: friend and foe for ischemic stroke. *J Neuroinflammation*. 2019;16:142. doi: 10.1186/s12974-019-1516-2

44. Hess DC, Hoda MN, Bhatia K. Remote limb perconditioning [corrected] and postconditioning: will it translate into a promising treatment for acute stroke? *Stroke*. 2013;44:1191–1197. doi: 10.1161/strokeaha.112.678482
45. Yang J, Shakil F, Cho S. Peripheral mechanisms of remote ischemic conditioning. *Cond Med*. 2019;2:61–68.
46. Chen C, Jiang W, Liu Z, Li F, Yang J, Zhao Y, Ran Y, Meng Y, Ji X, Geng X, et al. Splenic responses play an important role in remote ischemic preconditioning-mediated neuroprotection against stroke. *J Neuroinflammation*. 2018;15:167. doi: 10.1186/s12974-018-1190-9
47. Valsecchi V, Laudati G, Cuomo O, Sirabella R, Annunziato L, Pignataro G. The hypoxia sensitive metal transcription factor MTF-1 activates NCX1 brain promoter and participates in remote postconditioning neuroprotection in stroke. *Cell Death Dis*. 2021;12:423. doi: 10.1038/s41419-021-03705-9
48. Offner H, Vandenbark AA, Hurn PD. Effect of experimental stroke on peripheral immunity: CNS ischemia induces profound immunosuppression. *Neuroscience*. 2009;158:1098–1111. doi: 10.1016/j.neuroscience.2008.05.033
49. Hoda MN, Siddiqui S, Herberg S, Periyasamy-Thandavan S, Bhatia K, Hafez SS, Johnson MH, Hill WD, Ergul A, Fagan SC, et al. Remote ischemic perconditioning is effective alone and in combination with intravenous tissue-type plasminogen activator in murine model of embolic stroke. *Stroke*. 2012;43:2794–2799. doi: 10.1161/STROKEAHA.112.660373
50. Shimizu M, Tropak M, Diaz R, Suto F, Surendra H, Kuzmin E, Li J, Gross G, Wilson G, Callahan J, et al. Transient limb ischaemia remotely preconditions through a humoral mechanism acting directly on the myocardium: evidence suggesting cross-species protection. *Clin Sci (Lond)*. 2009;117:191–200. doi: 10.1042/CS20080523
51. Cappelli C, López X, Labra Y, Montoya M, Fernández R, Imarai M, Rojas JL, Miranda D, Escobar A, Acuña-Castillo C. Polymyxin B increases the depletion of T regulatory cell induced by purinergic agonist. *Immunobiology*. 2012;217:307–315. doi: 10.1016/j.imbio.2011.10.006
52. Beers DR, Henkel JS, Zhao W, Wang J, Huang A, Wen S, Liao B, Appel SH. Endogenous regulatory T lymphocytes ameliorate amyotrophic lateral sclerosis in mice and correlate with disease progression in patients with amyotrophic lateral sclerosis. *Brain*. 2011;134:1293–1314. doi: 10.1093/brain/awr074
53. Shi L, Sun Z, Su W, Xu F, Xie DI, Zhang Q, Dai X, Iyer K, Hitchens TK, Foley LM, et al. Treg cell-derived osteopontin promotes microglia-mediated white matter repair after ischemic stroke. *Immunity*. 2021;54:1527–1542.e8. doi: 10.1016/j.immuni.2021.04.022
54. Krasemann S, Madore C, Cialic R, Baufeld C, Calcagno N, El Fatimy R, Beckers L, O'Loughlin E, Xu Y, Fanek Z, et al. The TREM2-APOE pathway drives the transcriptional phenotype of dysfunctional microglia in neurodegenerative diseases. *Immunity*. 2017;47:566–581.e569. doi: 10.1016/j.immuni.2017.08.008

SUPPLEMENTAL MATERIAL

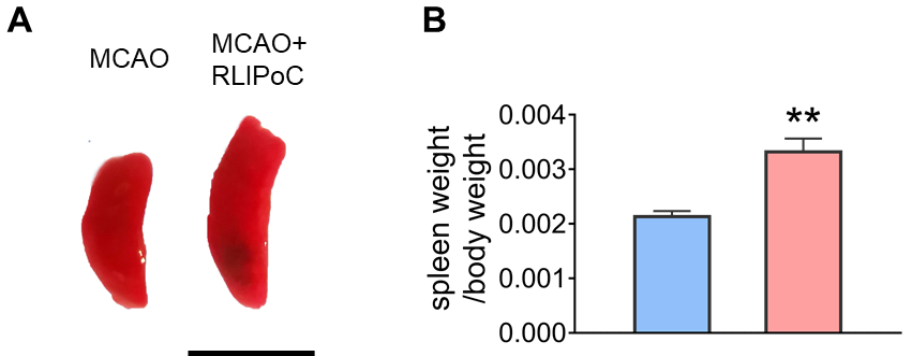

Figure S1. RLIPoC enhanced the ratio of spleen mass to body weight on day 3 after MCAO. Scale bar = 10 mm. Student's t test, **P < 0.01 versus MCAO. n = 6 per group.

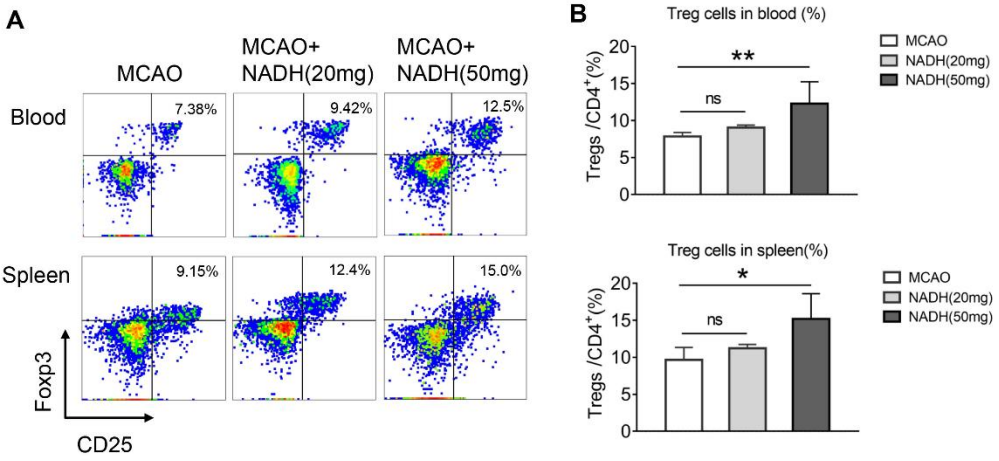

Figure S2. Tregs abundance of blood and spleen in mouse treated with different dosages (i.p. 20 or 50 mg/mouse) NADH within one hour after MCAO, and the mouse was sacrificed at 3 days after NADH administration. One-way ANOVA with Bonferroni's post hoc test. *P < 0.05, **P < 0.01; ns, not significant. n = 5–6 per group.

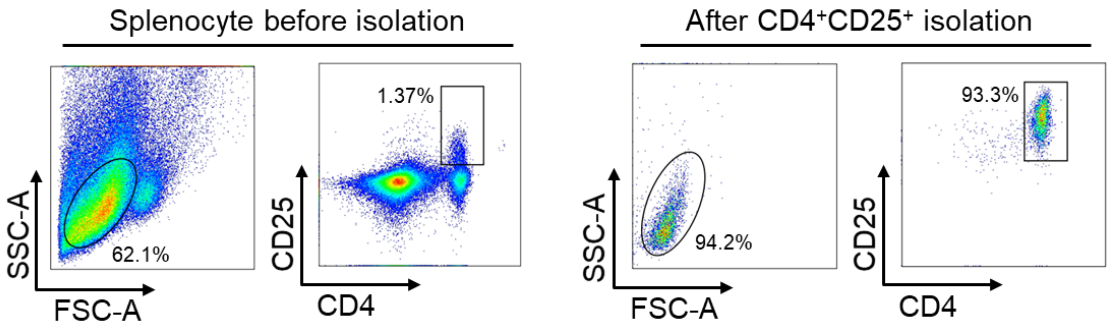

Figure S3. High purity $CD4^+CD25^+$ Tregs were magnetically isolated from the spleen of donor mice.

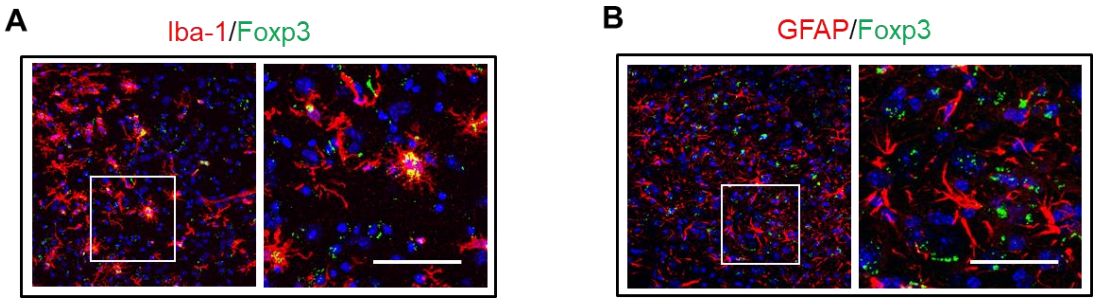

Figure S4. Iba-1+ microglia/macrophages were in close proximity to EGFP-tagged Tregs in the peri-infarct area. Scale bar = 50 μm.

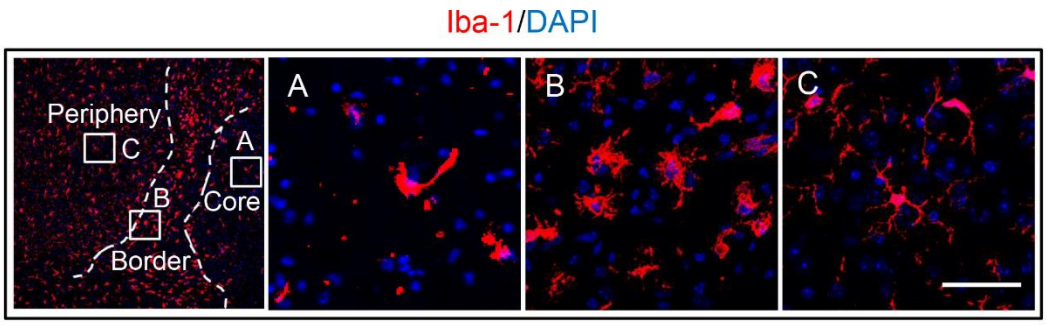

Figure S5. The different regions of infarct were determined by the accumulation and morphology of Iba-1+ microglia/macrophages. Scale bar = 50 μm.